3 Testing materials, equipment and methods

3.1 Introduction

With the aim of achieving the project objectives raised in Chapter 1 and Chapter 2, it was essential to carry out some careful decision making, planning and designing of the experimental methods, equipment and testing materials that were required for use in this project. It was also imperative to make use of the existing apparatus and facilities effectively to reach the project targets. This chapter outline the selection of testing materials, use of testing equipment, development and modifications made to the equipment and the techniques used in the work in this thesis.

3.2 Laboratory made paper

3.2.1 Pulps

3.2.1.1 Bleached Radiata Pine

It was essential to use a pulp that is currently used for paper manufacturing in this project. Radiata pine (*pinus radiata*), sometimes referred as "sapwood tree" is the principal softwood grown in the plantation forests of Australia, Chile and New Zealand. The radiata pine soft wood has the advantage of fast growth rate and it is currently used for the manufacture of a wide range of paper grades. Radiata pine has been graded according to a number of different grading rules and compared to other softwoods available around the globe.

A great deal of work on the characterisation and performance of radiata pine pulp fibres has been done by Kibblewhite and co-workers (Kibblewhite 1982; Kibblewhite, Bawden *et al.* 1995; Evans, Kibblewhite *et al.* 1997). The tensile index, stretch and TEA index of hand sheets made from radiata pine are known to increase with decreasing fibre coarseness at a given level of apparent density (Kibblewhite, Evans et al. 2002).

In this thesis, bleached market kraft pulps from New Zealand radiata pine, categorised as high, medium and ultra-low coarseness, were used in the laboratory sheet

preparation. The pulp was supplied as dry-lap sheets, courtesy of Dr. Paul Kibblewhite of the Pulp and Paper Research Organisation (PAPRO) of New Zealand. Optical micrographs of the fibres are shown in Figure 3.1.

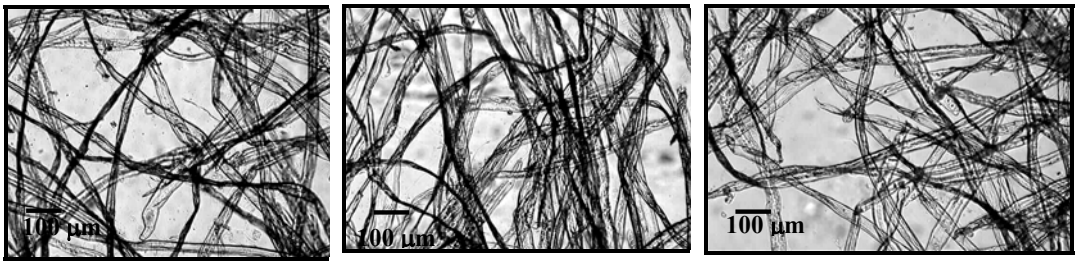

High coarseness **Medium coarseness** **Ultra-low coarseness**

Figure 3.1 Optical microscopic images of rewetted unbeaten, High, medium, ultra-low coarseness radiata pine pulp (x 50)

The details of the fibre dimensions are given Table 3.1.

Table 3.1 Details of pulp fibre dimensions (Wahjudi, Duffy et al. 1998)

		Fibre cross-section dimensions				
Pulp Category (Ave. Coarseness)	**Fibre length* (mm) FS200**	**Width + thickness µm**	**Wall area µm²**	**Wall thickness µm**	**Width: thickness ratio**	**Relative fibre number**
High	2.60	40.9	202	3.57	3.12	76
Medium	2.24	39.3	177	3.11	3.48	100
Ultra-low	1.88	39.4	169	2.96	3.63	125

***Length weighted fibre length**

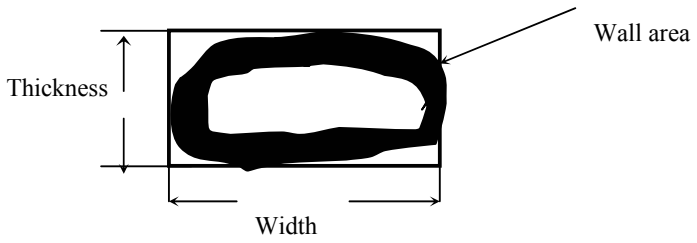

The measurements of fibre cross sectional dimensions, thickness, width, wall area and wall thickness shown in Table 3.1 were determined by Wahjudi *et al* using the image analysis method of Kibblewhite and Baily (1988). The area of the minimum fibre cross-section bounding rectangle is given by fibre-width x fibre thickness. The length weighted fibre lengths were determined using a Kajaani FS-200 using TAPPI method 271 pm-91 (Wahjudi, Duffy *et al.* 1998). The fibre coarseness is defined as the dry fibre mass per unit length. The fibre coarseness is the product of the fibre wall area x the density of the cell wall. It can be seen from the data in the table that the fibre coarseness is reduced as the fibre length is reduced. The relative fibre number shown in the table is the relative number of fibres in a unit mass of pulp and this was determined from the reciprocal of the product of length x wall area. It has been considered that the fibre width:thickness ratio is an indicator of the collapse potential of the dried and re-wetted fibres (Wahjudi, Duffy *et al.* 1998). Therefore, the collapse potential for the ultra-low coarseness fibres is greater than that of high or medium coarseness fibres and sheets made from ultra-low coarseness pulp may be expected to be well-consolidated even without refining.

3.2.1.2 Unbleached pulps

Some unbleached pulps also were used for additional measurements that were carried out to validate the method described in chapter 6. These were a never-dried unbleached radiata pine pulp, an unbleached eucalypt kraft pulp, unbleached NSSC pulp (Neutral Sulphite Semi Chemical). A mixture of unbleached radiata pine & eucalypt kraft pulp and a mixture of NSSC & unbleached radiata pine pulp were also used in laboratory handsheet preparation.

3.2.2 Disintegration and refining

The equilibrium moisture contents of the dried pulps were determined according to TAPPI standard T 550 om-98. The required amount of each pulp sample was soaked in deionised water for about 6 hrs and then torn into small pieces each of about 3 cm^2 in size. The pulps were disintegrated as described in TAPPI standard T 205 sp-95 until all fibre bundles were well dispersed.

Refining is a major means of improving the mechanical properties of paper. It is a mechanical treatment involving compression and shear of the chemical pulp fibres that

makes changes in fibre properties and consequently in sheet properties. The mechanics behind the process of refining pulp in commercial paper mills are complex and not well understood. Although a Valley beater used for the refining of pulp in this study does not exactly simulate commercial refining, it was the only laboratory refiner that was available that could handle the pulp masses required for this investigation.

The pulps used in this study were refined in a Valley beater according to TAPPI standard T200 om-89. The Canadian Standard Freeness (CSF) measurement was used as an index to estimate the degree of beating and this was measured to TAPPI standard T227 om-94. A master beating curve of CSF freeness against time was created, as specified in the standard, for each pulp as shown in Figure 3.2.

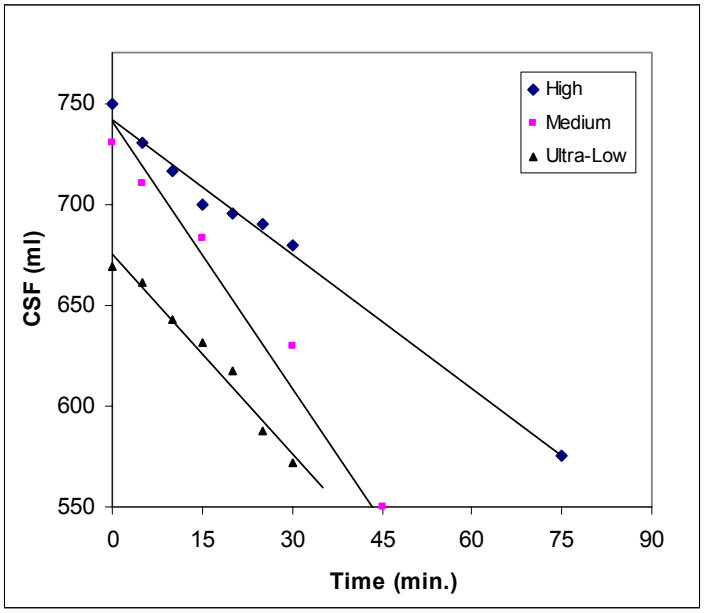

Figure 3.2 Beating curves for the bleached radiata pine kraft pulps used in this study

Figure 3.3 shows optical micrographs of the medium coarseness fibres after various levels of refining. These images clearly show the torn fibre surface and partially removed fibrils resulting from the mechanical action in refining. It is also clear that increased refining has increased the fibrillation of the fibre surface.

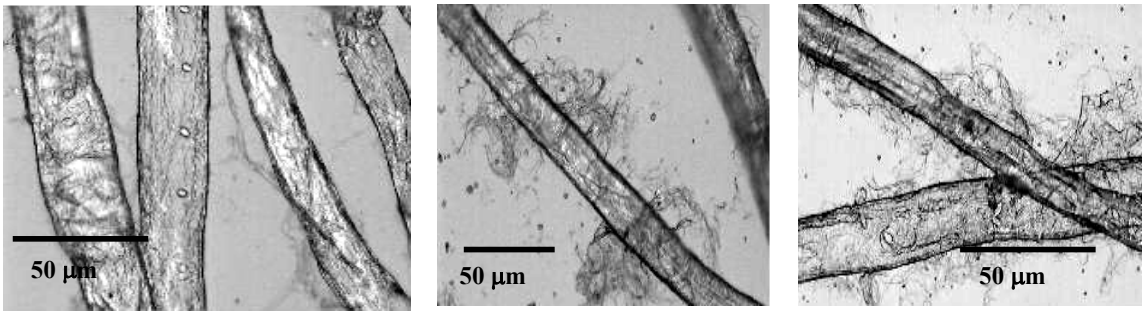

(a). Unbeaten (b). Medium beaten (c). Heavily beaten

Figure 3.3 Optical micrographs of medium coarseness fibres (a) unbeaten (b) beaten for 30 minutes (c) beaten for 60 minutes

3.2.3 Formation of laboratory sheets

The laboratory sheets used in this project were formed using a Moving Belt Sheet Former (MBSF). This machine was initially designed as a drainage tester and it can produce similar drainage conditions to those occurring on some commercial paper machines (Raisanen, Paulapuro *et al.* 1995). This machine can also produce sheets with

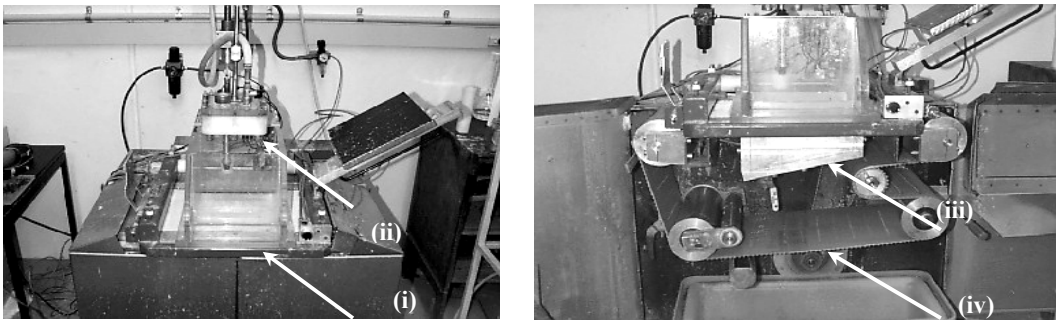

(a) **(b)**

Figure 3.4 Top and side views of Moving belt sheet former (MBSF) The image (a) shows the sheet-forming chamber (i) and agitation head (ii) and image (b) shows vacuum box (iii) and cogged belt (iv).

z-direction structure similar to some commercial papers. Another advantage of using the MBSF is its ability to produce larger isotropic sheets (220x220 mm^2) compared with a conventional British handsheet machine. The sheet making performance of the machine has been significantly improved by a number of recent modifications.

Images of the MBSF taken from the top (a) and side (b) are shown in Figure 3.4. A detailed description of construction, operations and modifications of MBSF can be found in (Xu and Parker 2000) and Mitchell *et al* (Mitchell 2002).

With the pinus radiata pine pulps, the stock that was prepared for sheet making required considerable dilution to obtain good sheet formation, due to the pulp's tendency to heavily flocculate at the normally used concentration (~ 0.3%). The concentration that gave good formation was found to be 0.07% and all the samples were made with this concentration. A constant vacuum pulse rate of 80 Hz and a constant ramped vacuum profile were used to form all sheets. The vacuum was set to 6 kPa. The constant pulse rate was obtained by the moving cogged belt with rows of holes punched 13mm apart. After forming the sheet, a pneumatic couching device attached to the MBSF was used to press the wet sheet onto a blotter to reduce the excess water. A metal plate was kept under the formed sheet and the wire to obtain uniform pressing.

3.2.4 Wet pressing

After the newly formed sheet was couched from the pneumatic press, the sheet and its attached blotter was withdrawn from the forming wire of the MBSF and placed on a press felt. Then a "Fibre Tech" laboratory sheet roll press was used to press the newly formed wet sheet to improve the consolidation of fibres and to further reduce the water content.

When pressing with a roll press, the water flow and the densification of the sheet is expected to more closely simulate a commercial paper machine press than a normal laboratory sheet press. A metal drying plate was applied on the other side of the hand-sheet and another pressing felt was added on top of the drying plate. Then the sandwich consisting of the top felt, blotter, handsheet, drying plate and bottom felt was passed through the press at a set pressure. The sheets formed from the medium coarseness fibres were wet pressed with one of two different wet pressing levels. A low level of pressing was performed using a 2.0 bar gauge pressure and a high level of pressing was obtained using a 6.0 bar gauge pressure. Sheets made from the other two pulps were only pressed with the 2.0 bar gauge pressure. For low level pressing, the stack was passed twice through the roller press and for high level pressing the stack was passed

through once at 2.0 bar pressure and then passed through twice at 6.0 bar pressure. In order to obtain uniform pressing, the felts were conditioned before they were added to the sandwich. To condition the felts, they were soaked in water for few minutes and passed through the roller-press once at low pressure and twice at higher pressure.

3.2.5 Sheet drying and storage

The nature of the drying of newly formed sheet greatly influences the mechanical properties of paper. The fibres that are used in papermaking shrink during drying and the amount of shrinkage is dependent on the degree of swelling of the fibres and the degree of restraint under which the sheets are dried. Therefore following a consistent procedure in drying the handsheets is of utmost importance in producing sheets with reproducible mechanical properties.

The procedure followed here was to place the wet laboratory made sheets in drying squares to dry under restraint in a standard conditioned room at 23^{o}C constant temperature and 50% RH. The sheets were dried for 24 hours and then removed from the drying racks and the attached drying plate. The sheets were then kept in the conditioned room for long-term storage.

3.2.6 Thickness measurements

The measurement of sheet thickness was necessary to calculate the apparent density and cross sectional area of the samples. The combination of sheet thickness and the sheet grammage gives a measure of sheet's apparent density and the cross sectional area is necessary for stress calculations.

However, unlike most other solid materials the measurement of thickness in paper is not straightforward. This is mainly due to the porous structure of the paper and the measurement of sheet thickness can be affected by the compressibility and roughness of the sheet. Therefore following a set standard in the measurement of thickness is necessary to obtain a repeatable measurement.

In this investigation, thickness was measured using a "Messmer" digital micrometer according to AS/NZS 1301.426s:1994 with standard metal platens. The thickness of

nine local areas, selected by dividing the square sheet into a 3x3 grid was measured and the average was taken to determine the thickness. Each of these nine measurements was the average of three measurements taken from the local area. Thickness was measured both for the handsheets and for the commercial papers.

3.3 Commercial papers

"Reflex" copy paper and unbleached sack kraft manufactured by PaperlinX, and 100% recycled, plaster liner board manufactured by Visy Paper were the commercial papers used in this investigation. Table 3.2 shows the grammage and thickness of these papers.

Table 3.2 Basic physical properties of commercial paper samples

Paper	**Air-dry Grammage (g/m^2)**	**Thickness (μm)**
"Reflex" copy paper	80	102
Sack kraft	81	163
Plaster liner	190	190

Other commercial papers tested for further evaluation of the new test method described in Chapter 6 are listed in APPENDIX D.

3.4 DENT sample preparation

Deep double-edge notched tension (DENT) geometry specimens (see Chapter 2) were required for fracture toughness measurements using both the EWF and the proposed cyclic techniques (see Chapter 6 for details). To obtain reliable results it is necessary to cut samples with sharp clean notches and consistent dimensions. A slight variation at the crack tip or some pre-straining of the ligament could give inaccurate and inconsistent values and hence careful sample handling is also required to avoid any damage to the specimens.

3.4.1 Cutting die

Designing a cutting jig that can be used to cut clean notches and can also make specimens rapidly was a difficult task during the initial stages of the project. A cutting jig, similar to that described previously (Seth, Robertson *et al.* 1993), was initially

tested for this purpose. The jig consisted of two sharp tool steel blades clamped in between two metal plates (see Figure 3.5 (a)). The distance between the two blades was adjustable according the ligament length that was required. Instead of placing the jig vertically over the specimen and hitting it manually with a hammer, as was carried out in Seth *et al'*s work, the jig was mounted on a one sided fly press to apply a constant vertical cutting force.

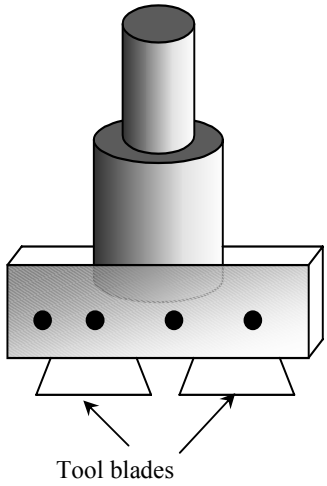

Figure 3.5(a). Cutting jig that was tested for making edge notches on DENT samples

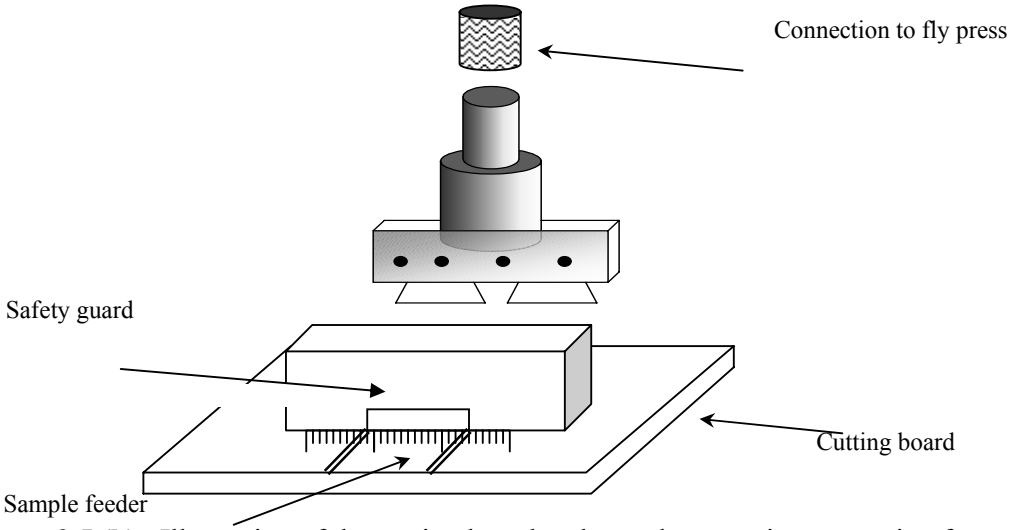

Figure 3.5 (b). Illustration of the cutting board and sample set up in preparation for cutting a notch

The set up that was built to cut notches with the jig is illustrated in Figure 3.5 (b). The specimens were backed by smooth cardboard to give a cushioning effect when the notches were introduced. Although the jig produced clean, reproducible, notches in the

specimens, there were a few drawbacks in the set-up and use of the jig. One drawback was the amount of time required to cut a set of specimens sufficient to measure one EWF fracture toughness value. Although cutting a few samples together to introduce notches was potentially possible, in practice only one specimen was cut at a time to ensure the uniformity of the notches. Another time-consuming exercise was aligning the sample on the cutting board to introduce symmetrical notches in the middle of the samples, which have different ligament length. An additional drawback was that the fly press could not be moved to the test room. Therefore the samples had to be re-conditioned after cutting, which was a very time-consuming process.

A new cutting die was designed to produce 10 DENT samples with different ligament lengths, from a sheet made from the MBSF, in a single cut. A die-press machine to do the cutting was installed in the conditioned test room. These steps overcame the main problems associated with the previous sample preparation method. A sketch and a photograph of the die are shown in Figure 3.6.

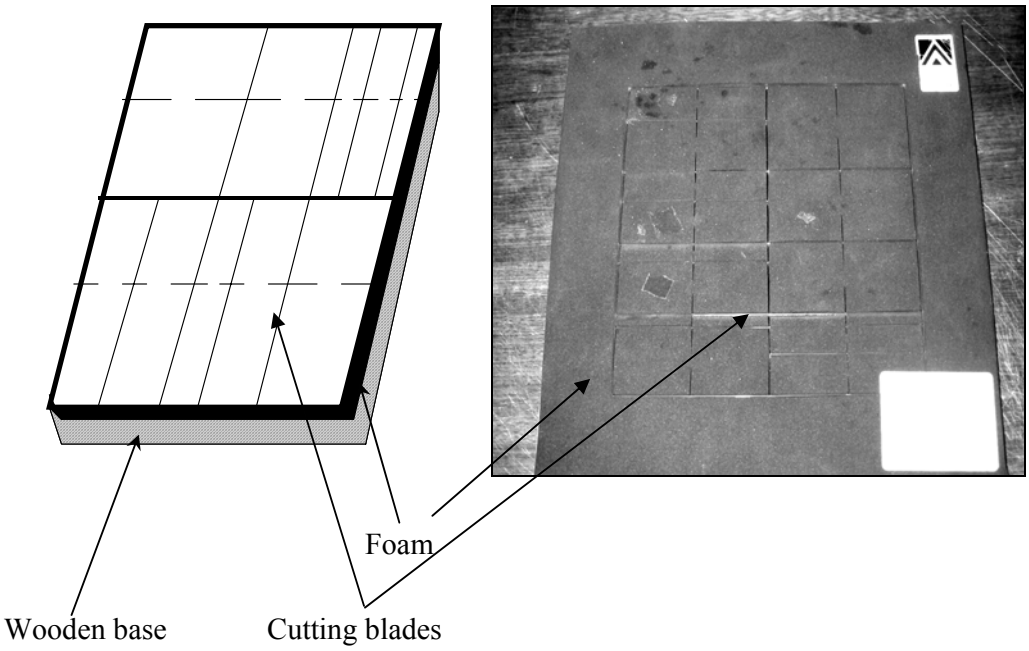

Figure 3.6 Multi-specimen (DENT) cutting die

The cutting area of the die was 210 x 200 mm^2. Spring steel was used to make the cutting blades and these blades were mounted onto a wooden base. The wooden base was covered with a 9 mm thick foam pad and the cutting blades were embedded in the foam. The foam pad protected users from coming into contact with the blades. During the down-stroke of the press, the foam is compressed, exposing the blades. After release of the press, the relaxation of the foam pushes the blades out of the specimen. This die was designed to cut 10 DENT samples, each with a different ligament length. The ligament lengths were as follows: 14.1, 12.1, 10.8, 9.3, 9.0, 7.7, 6.1, 5.1, 4.0 and 3.3 mm.

3.4.2 Press

A GSB-1 series hydraulic swing beam press was used to press the cutting die onto the paper to stamp out the specimens. An image of the press is shown in Figure 3.7

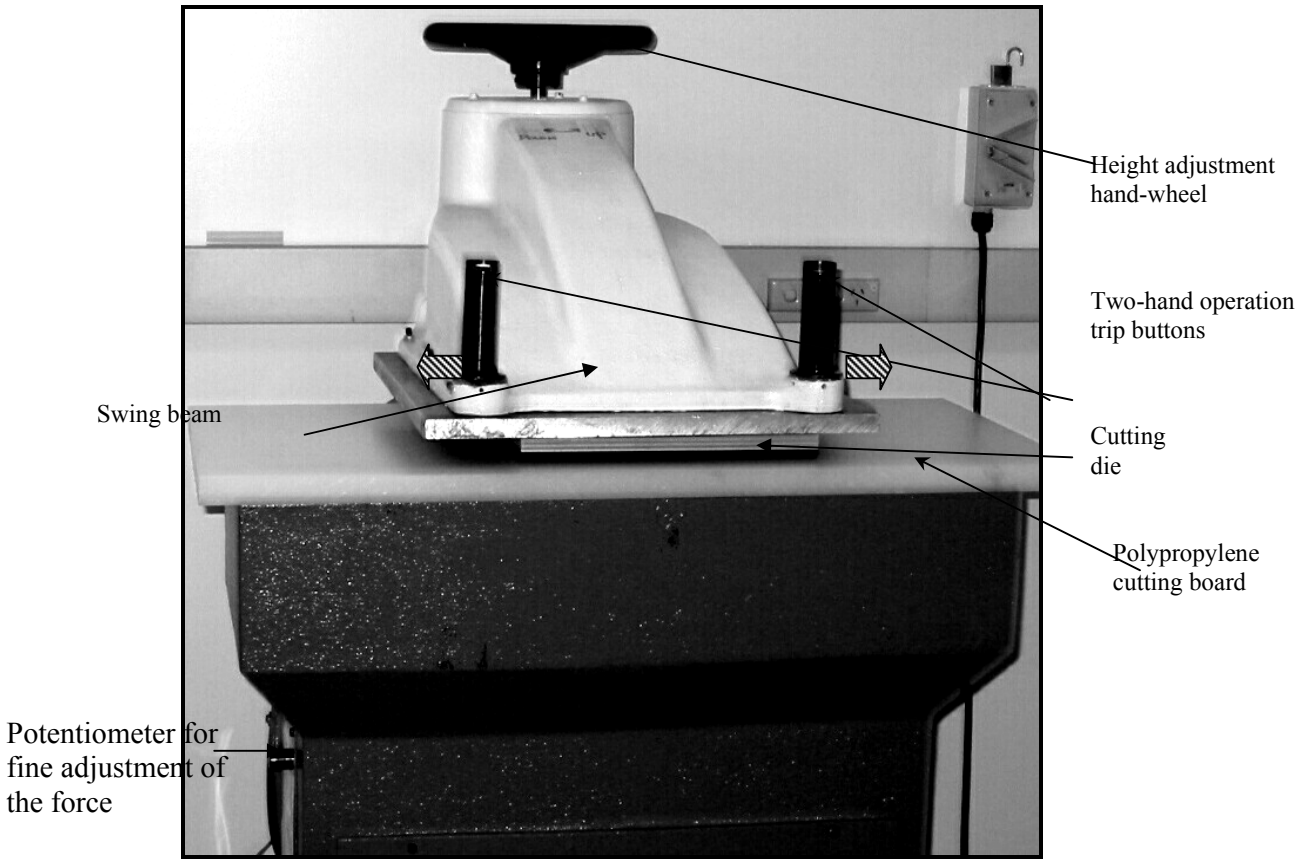

Figure 3.7 GSB-1 series hydraulic swing beam press

The press consists of an integral cast iron base, a high strength steel column and a lightweight cast steel swing beam mounted on the column. The steel column is located in precisely machined guide bearings in the base. The base is used as the sump for the hydraulic oil and also houses the hydraulic unit. An electric motor, driving the pump through a flywheel mounted on the motor shaft, provides the power to the hydraulic unit. The hydraulic cylinder is attached to the lower end of the column. A powerful spring is connected around the piston rod to release the beam after cutting has been completed. The hand-wheel at top of the beam allows the height of the beam above the working table to be changed.

When the trip buttons on the beam are activated, hydraulic oil is directed to the cylinder forcing the beam downward and into contact with the back of the cutting die, pressing it on the paper placed on the polypropylene cutting table. A potentiometer mounted on the machine enables the downward movement to be precisely adjusted. At the end of the cutting stroke the beam is returned to the pre-set upper position by the spring. The advantage of this press is its ability apply a uniform force onto the cutting die and that it self-releases after completing the cutting.

3.5 Testing environment

It is required that the paper and paper-board samples establish a reproducible equilibrium moisture content between the sample and an environment of specified temperature and relative humidity before any mechanical testing is conducted. It is considered that the equilibrium is reached when the two consecutive weightings of a sample, which have been carried out at an interval of time of not less than one hour, do not differ by more than 0.1 % (APPITA P414m – 86).

3.5.1 Standard conditioned test room

The standard atmosphere for testing pulp, paper and paperboard is (23 ± 1)^{o}C and (50 ± 2) % RH. All the tests were carried out in a conditioned test room that operated better than the AS 1301.415s-1998 specified tolerance and was controlled to (23±0.1) ^{o}C and (50±1)% RH.

3.5.2 Humidity Generator and relative humidity measurements

When tests were carried at varying relative humidity levels, a humidity generator (HD-100-TC) manufactured by "Tecnequip" was used. The humidity generator has the ability to supply conditioned air at the standard temperature of 23^{o}C and at any set relative humidity from 1 to 99 % and provided conditioned air streams at a rate of 96 litres per minute. The humidity generator was computer controlled and any sequence of humidity levels could be set.

The environmental conditions (humidity and temperature) in a workspace were independently monitored using a "Vaisala" humidity probe (model HMI-33). This probe was regularly calibrated with saturated salt solutions to maintain its accuracy. The moisture content of the sample at a given humidity was estimated according to ISO 287-1985 (E).

3.5.3 Sample conditioning

The samples that were to be tested under different humidity levels were stored in the conditioned test room prior to the testing and then they were pre-conditioned at 90% RH for 5 hours in a sealed humidity chamber (see Figure 3.8) that enclosed the whole testing equipment, to remove dried in strains and to obtain a constant de-aging condition.

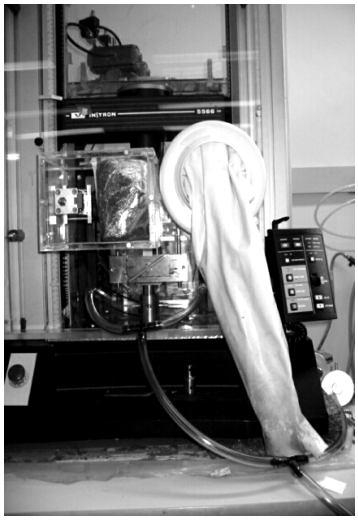

Figure 3.8 The sealed humidity chamber that was used to carryout tests at environments other than 23 ^{o}C and 50% RH.

The pre-conditioning of samples also reduced any errors associated with the hysteresis of the equilibrium moisture content. The hysteresis in equilibrium moisture content is due to the differences in the absorption and desorption of moisture in paper at a given relative humidity when coming from a higher or lower humidity, respectively. When the tests were carried out at 90% RH, a further 5 hours of conditioning was carried out after the samples were pre-conditioning, giving a total of 10 hours of conditioning. For tests at other levels of RH, samples were conditioned for a further 10 hours at the testing environment.

3.6 Measurements of mechanical properties of paper

3.6.1 EWF Fracture toughness

The Essential Work of Fracture (EWF) technique (Seth, Robertson *et al.* 1993; Seth 1995) was used as a one method of estimating Fracture Toughness (FT). The EWF test is conducted using the DENT geometry, which consists of two edge notches cut on opposite side of the sample, leaving a central ligament (L) across which fracture occurs during the test.

3.6.1.1 Clamps

In the EWF method, DENT specimens containing varying ligament sizes are strained to failure and the total work of fracture is estimated from the area under the load-extension

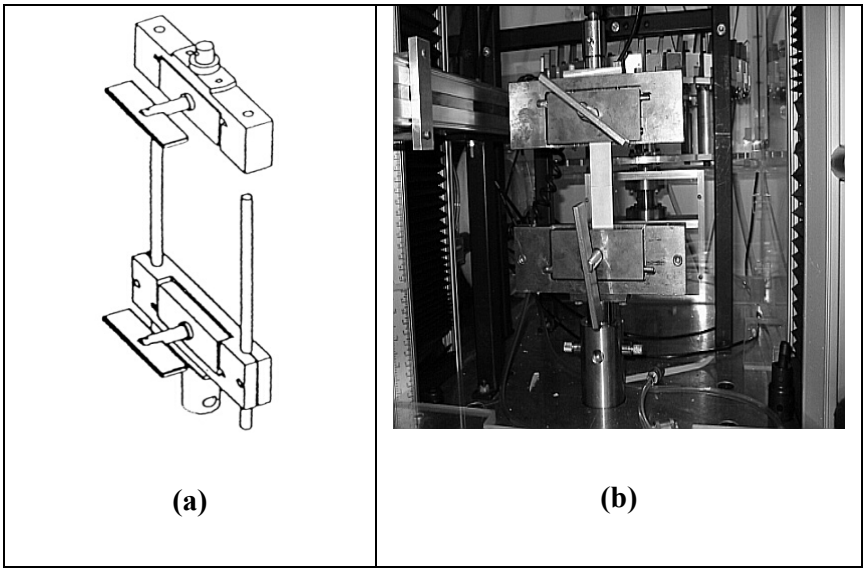

Figure 3.9 **(a)** A sketch of line type clamps (Seth, 1995) and **(b)** and image of the clamps without linear guide rods

curve. To satisfy the conditions prescribed in EWF method, the ligament should remain in plane stress. If the width of the sample is large then it is difficult to uniformly clamp the sheet along its width. This causes problems in maintaining uniform stress in the plane of the sheet. A specially designed clamping rig similar to that described by Seth (1995) was used to overcome this problem. This was a pair of line type clamps, where one clamp encapsulated two low-friction linear bearings and can move along two linear guide rods. The clamps were mounted on an Instron, (load frame type 5566) universal testing machine.

The Instron tester is very rigid and quite accurate and is able to resolve 1μm displacement and 1mN changes in load. Figure 3.9a shows a sketch of the line clamp and Figure 3.9b shows an image of the line type clamp rigidly connected to the Instron universal tester. These clamps were designed to test samples with a width up to 100 mm.

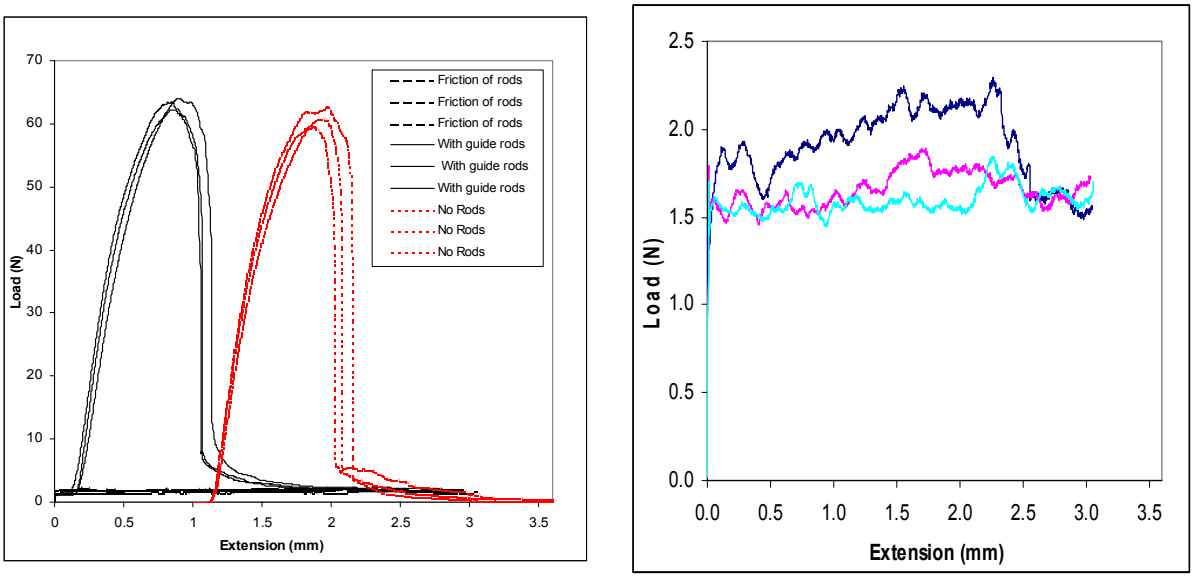

(a) **(b)**

Figure 3. 10 **(a)** Load extension curves obtained from DENT samples with L=14.1 mm. The curves with solid lines were obtained with guide rods, the curves with dotted lines were obtained without guide rods (these have been shifted to the right to make them easier to see). The tests carried out with guide rods alone (no sample) are shown in broken lines. **(b)** An enlarged view of the fictional force profile of the guide rods alone

The reason for having linear guide rods is to ensure that the specimen is loaded in plane stress. In previous work, it was confirmed that the effect of buckling in DENT specimens of paper is generally insignificant (Seth 1995). However, the guide rods can be useful when loading tough wide samples to avoid buckling and to ensure that the samples experience a tensile mode of fracture. The samples that were tested in the previous EWF work by Seth *et al* (1993) had ligaments up to 50 mm long. Since the specimen width should be at least three times the ligament length, the samples that were used in the previous study should have been at least 150 mm wide. Therefore the use of linear guide rods in the clamps for such samples is important. However, during our study the maximum sample width used was 60 mm.

Tests were carried out with and with out linear guide rods to see the effect of guide rods on load-extension curves, using different ligament lengths. Figure 3.10a shows typical load-extension curves obtained from a high coarseness radiata pine sample refined for 75 minutes. The sample ligament length was L=14.1 mm, which was the largest ligament length used in this work. The figure shows the load extension curves obtained with guide rods, without guide-rods (shifted to the right) and without a sample to obtain the friction of the guide-rods alone. A magnified view of the friction of the guide rods is shown in Figure 3.10b. The average friction of the guide rods is about 1.6N. Extreme care was taken during the tests in both instances to make sure that the clamps were rigidly mounted to the Instron and the clamp jaw faces were parallel when the samples were being strained. Table 3.4 shows the average maximum load and area under the load-extension curve obtained with and without the guide rods. The frictional forces were not subtracted in the values shown in Table 3.4 when the tests were carried out with guide rods. These tests were carried out on 12 samples for each set up and the results on both occasions were found to be consistent and the differences were well within the measurement uncertainty. The errors indicated with the values were obtained from 95% confidence intervals. The increase in the maximum load and the area under the curve, when measurements were carried out with the rods, is due to the friction of the guide-rods.

Table 3.4 Results obtained with and without guide rods in the fracture toughness rig

Test without guide-rods		**Test with guide rods**	
Ave. Maximum Load (N)	**Area under the curve (N.mm)**	**Ave. Maximum Load (N)**	**Area under the curve (N.mm)**
59.2 ± 2.4	42.1 ± 2.0	61.3 ± 2.7	45.8 ± 1.8

In results obtained with the guide rods, the subtraction of frictional forces is required. If the frictional force is constant this will be an easy task. However, there were some differences (~ ± 0. 3N) in the friction of guide rods from test to test and continuous lubrication of guide rods was also required to maintain a constant friction. These slight changes in the friction were causing problems in the sensitive estimation of area under the curve from the load-extension curve. Therefore the EWF tests and cyclic tests (see Chapter 6) were carried out with out the linear guide rods. The effect of removing the guide rods was found to be insignificant as shown in Figure 3.10a and Table 3.4.

3.6.1.2 Test conditions

It has been claimed in the literature that stable crack growth is important to obtain accurate EWF measurements (Yu and Karenlampi 1997). A short specimen, a rigid test system and a slow cross-head speed help to obtain a stable crack growth. Accordingly, in the initial investigations, the span between the line clamps was set at 90mm and the Instron's cross-head speed was maintained at a slow elongation rate 2 mm/min.

Our test results suggested that even with these conditions, it was not possible to obtain stable crack growth at all combinations of sample, ligament length and elongation rate. However, subsequent investigations (see Chapter 6) showed that it was not necessary to have fully stable fracture to obtain an accurate measurement of EWF fracture toughness, provided that the stored elastic energy at fracture was not enough to completely fracture the sample. Despite these findings, the test conditions were maintained as described above, so that all the fracture toughness measurements in this study could be directly

compared with each other. The number of replicate tests for each data point was 15. This number was chosen to produce a reasonable mean value. An example for a EWF test carried out for ligament length L=7.7mm is given in Appendix A.

3.6.1.3 Cyclic load control fracture toughness testing and data analysis

During this thesis a new method has been developed to estimate the fracture toughness using cyclic loading of DENT samples. The maximum load in each cycle was increased until the sample failed. The unloading parts of the cycles did not contribute any information to the tests and so the unloading rate was set to 10 mm/min to speed up the tests. The details of the technique are given in Chapter 6 of the thesis. The data analysis of the cyclic test was a time consuming exercise if this was done manually. A Visual Basic macro programme was written (Conn and Wanigaratne 2001) and run through Microsoft Excel 2000 to automate the data analysis and to obtain the results within a few minutes (see Appendix B for source codes of the program).

3.6.1.4 The function of the macro programme

The data (time, extension & load) for 15 specimens were collected as ASCII raw data from the Merlin software, that is used to run the Instron, and saved into a single file. The initial function of the macro is to separate the tests into individual worksheets in Excel. Then the macro calculates the extension/time at each point along the load-extension curve averaged in three point groups, to identify the "peaks" and the "bottoms" of the cyclic curve. The values of the extension and load belonging to peak points are extracted from the data and the extension and load data points from the maximum load to the end of the last cycle are written in two separate columns with extension in one and the load in the other. These steps are carried out to construct the full load-extension curve from the peak points of the cyclic load-extension curve. The whole area under the full load-extension curve is calculated using the trapezium rule. The next task of the macro is to define the last cycle of the cyclic load-extension curve. The "bottom" point at the highest time defines the beginning of the last cycle. The extension and load data points starting from the corresponding final bottom point to the end of the test are written to two separate columns as extension and load to construct the final cycle. The area under the last cycle is calculated again using the Trapezium rule. Finally the total area and the area of the final cycle are displayed in an interface in Microsoft Excel. These steps are repeated automatically for all specimens and the

average values and their uncertainties, obtained from 95% confidential intervals, are displayed in the interface. Once the sample ligament length and the grammage are entered in the interface, the fracture toughness of the material is calculated. (See Appendix B for more details).

3.6.2. Tensile measurements

The Instron universal tester described earlier was used for all tensile tests in this study.

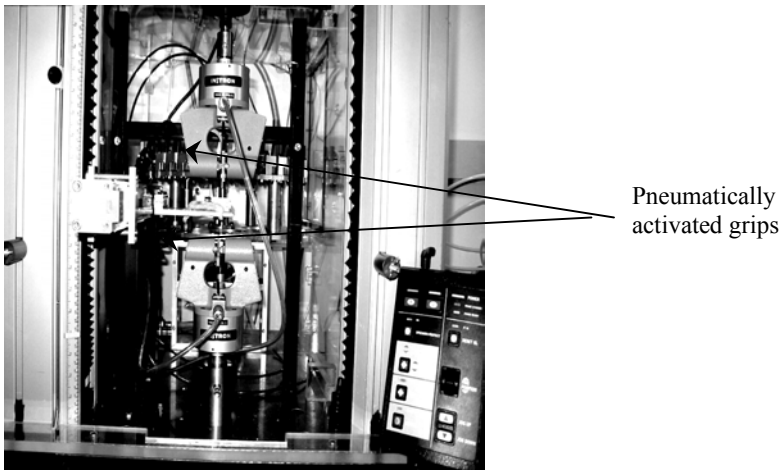

Figure 3. 11 Experimental set up for tensile measurements

Tensile test strips of 15 mm width were cut using a standard cutter (Messmer model F215). As shown in Figure 3.11, pneumatically activated grips operating at 400 kPa with line faces clamping the test specimens at a test length 100 mm was used to strain the samples. All the tests were carried out at elongation rate of 10mm/ minute. Tensile tests were performed in accordance with the ISO standard 1924-2:1994.

3.6.3. Zero-span tensile strength

The "zero span tensile test" is a technique that determines the tensile strength of the fibres within a sheet. In this test the grips that hold the specimen are brought together (zero span) and clamped such that the resultant tensile force is applied across a plane through the thickness of the sample. The standard methods that describe the zero span test (AS/NZS 1301.459rp – 1998, TAPPI T231 pm-95) call for the tests to be conducted on wet sheets. This is because it had been previously suggested that the zero span result depends on the inter fibre bonding and to eliminate this bonding the sheet should be

wetted. However, other studies indicate that bonding has insignificant effect on zero span tests and the argument of eliminating bonding by wetting the sample has no foundation (Seth 2001), (Gurnagul and Page 1989). In this study, the standard test method was followed, except that the sheets were tested dry. The tests were conducted using a Pulmac "Troubleshooter" zero-span tester.

3.6.4 Concluding remarks

It is obvious from the details given above that a collective contribution from all the methods and apparatus are required to carryout a detailed investigation of the fracture toughness of paper. The experimental results obtained by following these methods are given in rest of the chapters in this thesis.

4 Image Analysis of plastic deformation in the fracture of paper

4.1 Introduction

As detailed in Chapter 2, one of the fundamental problems that arises in the estimation of the fracture toughness of an elastic-plastic material like paper is the significant amount of plastic deformation that can occur in areas away from the Fracture Process Zone (FPZ). A brief summary of the mechanism that leads to the plastic deformation is given here.

When a tough, non-linear elastic-plastic material with a crack is strained, the material will offer resistance against the crack propagation. The resistance offered by the material against crack propagation is the fracture toughness. When large loads are applied to the material, it can yield not only in the area just ahead of the crack-tip (the Fracture Process Zone (FPZ)), but in areas away from the FPZ as well. In such circumstances the work that is consumed for plastic deformation in areas away from the FPZ is not a part of the fracture toughness, and hence needs to be excluded from the total work. The EWF technique is a method of separating the work in the FPZ from the work of plastic deformation. However, the EWF technique requires measurements of a large number of samples at many different ligament lengths in order to perform this separation. There is no direct or easily applicable method that can be used to estimate the work consumed in the outer plastic zone.

The original aim of using an image analysis technique was to obtain more information on the outer plastic region and also to see whether this information can be used to quantitatively estimate the work consumed for plastic deformation. If the work spent for the plastic deformation in the outer plastic zone can be successfully independently estimated, then the fracture toughness of the material can be obtained by subtracting this plastic work from the total work obtained from a single ligament DENT sample. This could significantly reduce the amount of time required for multiple ligament sample preparation, testing and analysis in the EWF or J-integral methods. Another advantage

would be that testing at a single ligament length would use much less sheet area than that generally required for a full EWF test. The other possible importance of the image analysis technique is that additional information could be acquired from this technique, such as the shape and extent of the outer deformation zone, which can be used to test the validity of the assumptions behind the EWF technique. Some of the pre-conditions of using the EWF technique are that: (a) the DENT specimen should yield completely before fracture (b) the deformation field around the ligament should have formed a uniform shape before fracture commences and (c) the plastic deformation work should scale with the ligament length squared.

4.2 Samples, apparatus and the technique

The samples used in this experiment were 80 g/m^2 "Reflex" copy paper manufactured by PaperlinX. A software package (Corel Draw 7.0) was used to design fine lines (250 μm apart) that were printed on the sample along the Machine Direction (MD) or the Cross machine Direction (CD) according to requirements.

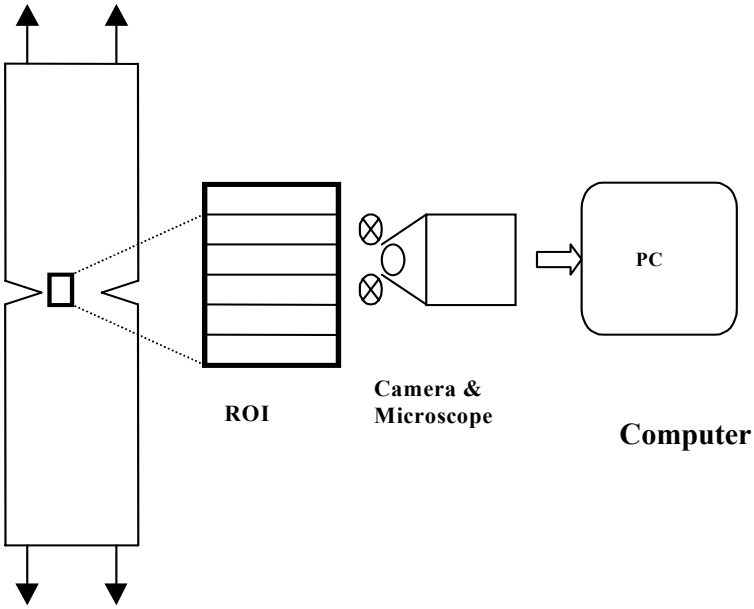

Figure 4.1 Experimental set-up for image capturing system

The image analysis technique essentially estimates the distance between fine printed lines (at a given position) from images captured before and after straining the sample. The distances were each an average of the distances between seven or eight lines in one

given image. Comparing the same image before and after straining allows the average strain to be estimated.

Figure 4.1 shows the experimental set up used for the image analysis. Images of a Region Of Interest (ROI) were captured using an OLYMPUS SZ40 microscope, a PULNiX TM-6CN CCD camera and a personal computer equipped with a MACH Series DT 3155 frame capture card, before and after straining in the Instron. The guidelines (see Figure 4.2) printed perpendicular to the fine lines were used to locate exact positions in the test pieces during image capture. It was necessary to remove the sample from the Instron to capture the images. This is because it is necessary to move the sample under the microscope in order to capture the series of images required to measure the whole deformation field. This was not possible while the sample was mounted vertically in the Instron.

A fundamental assumption of the EWF technique is that the outer plastic zone is circular or elliptical with diameter *L*. The ligament length *L,* of the DENT sample used in this experiment was 15 mm. To test the validity of this assumption, images were collected over an area that was larger than the expected size of the deformation zone.

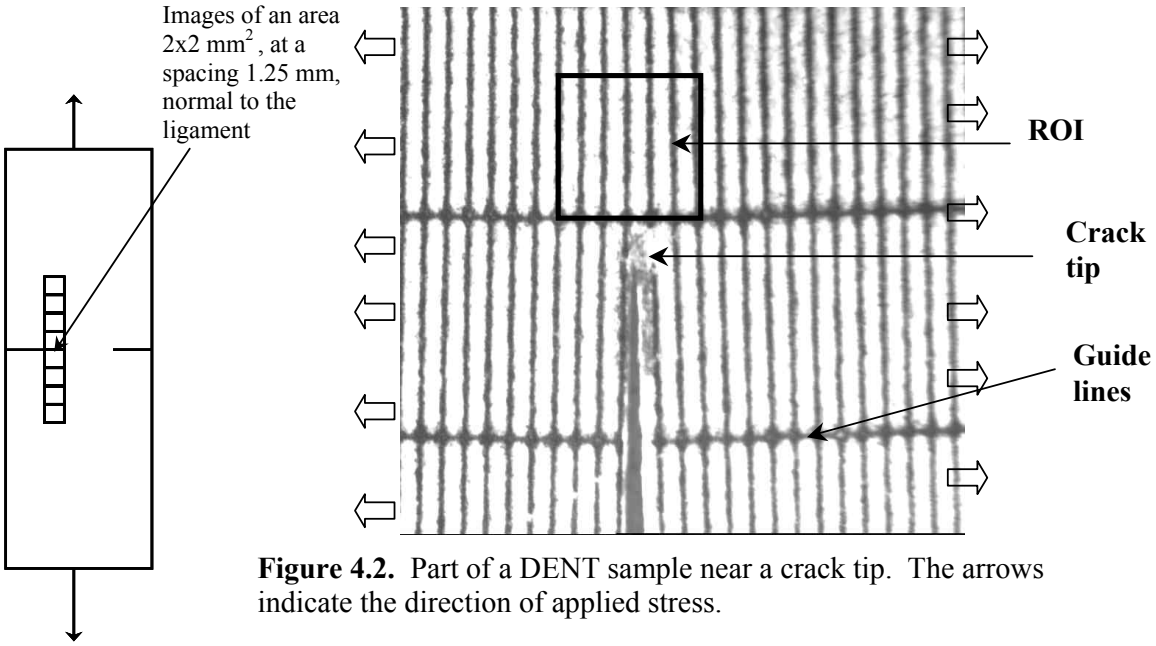

Figure 4.2. Part of a DENT sample near a crack tip. The arrows indicate the direction of applied stress.

To accomplish this task a series of images, at a spacing of 1.25mm, were captured along a 25mm line, normal to and centred on the ligament (see the left insert in Figure 4.2). The microscope magnification was set to capture images containing 7 or 8 lines (in an area of about 2x2 mm^2) so that the average line spacing could be obtained accurately.

Figure 4.2 illustrates a ROI near the crack tip of a sample. A typical captured image is shown in Figure 4.3. Optimas image-processing software was used to obtain an average gray scale value for each one pixel wide column, which was set perpendicular to the direction of the applied stress, and the whole image was converted to an intensity profile. Minima in the transformed profile represent the centres of the dark lines, where the gray-scale intensity is a minimum. The gray scale values were then inverted by subtracting them from the maximum gray scale value of 255 to convert the dark lines from valleys to peaks. The resulting data were exported as a text file. The centres of the peaks were obtained using a peak-fitting program "Peaksolve". Figure 4.4 shows a typical inverted gray scale plot obtained after processing the image in Figure 4.3, together with the fitted curve obtained from the peak-fitting program. It can be seen that the peak fits obtained were good and that the accuracy of the estimated peak centers was within ± 0.03 pixel. Averaging 7 or 8 peak centres further reduced the uncertainty of these values. Finally, with the aid of spreadsheet software, the average line spacing and its uncertainties were obtained from a fit of the peak positions.

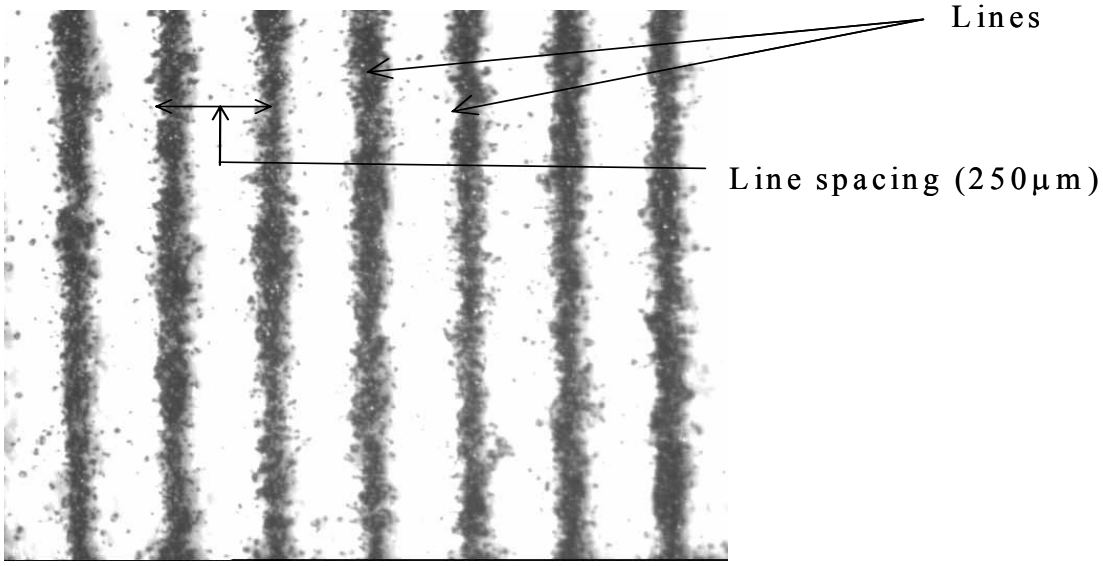

Figure 4.3. A typical image showing 7 lines. (Lines are 250 μm apart)

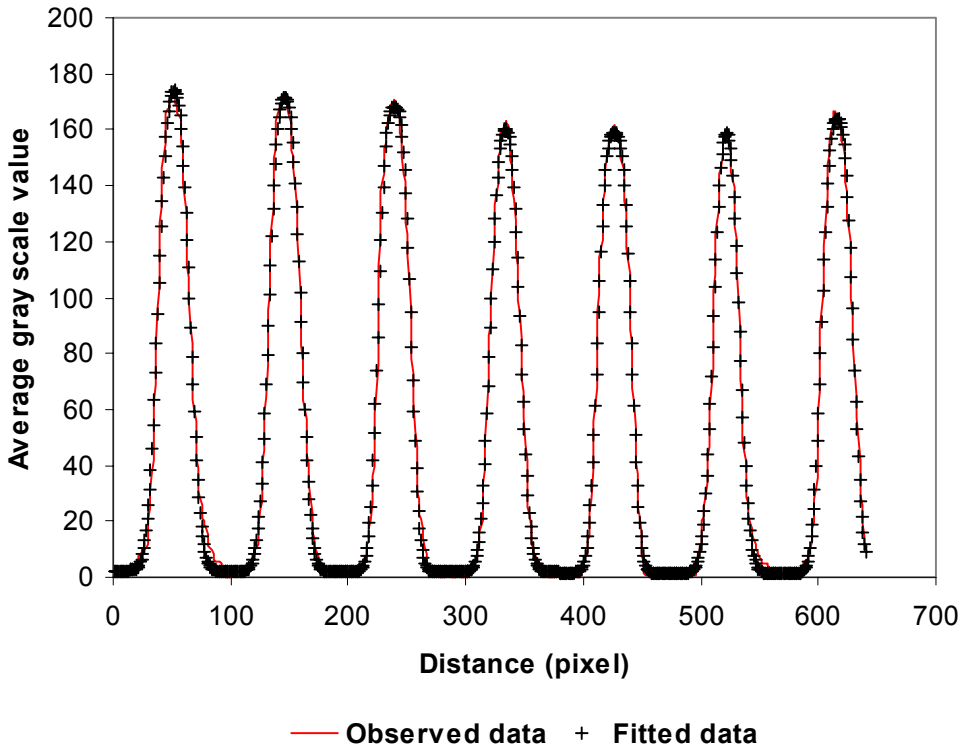

Figure 4.4. Inverted average gray scale plot for the image in Figure 4.3 (the crosses give the fitted curve)

4.3 Sample straining

The samples were strained using the grips for EWF testing described in Chapter 3. The cross-head speed of the Instron was set at 0.5 mm/minute. The vertical guide-rods were used in the rig during these tests to ensure that the sample is loaded in-plane. The friction due to guide rods was subtracted from the area under the load elongation curve during the analysis. The average breaking load of the sample was obtained by testing 12 test pieces and this value was used as a guide to decide when to terminate the straining process. A microscope was also used to observe the notch tip and to determine the critical point to stop straining before the crack began to propagate.

4.4 Calibration

To check the accuracy of the technique for determining strain, real-time images from the middle of a printed tensile test piece with 100 mm span were captured at a rate of 1.8 frames/second. The sample was commercial copy paper, strained in the CD direction at a strain rate of 0.5 mm/min (0.0083% per sec.). The lines were printed

normal to the applied stress. A comparison was obtained between the set linear strain rate (0.0083% per sec.) and the experimental strain rate determined by image analysis.

Figure 4.5 shows the results obtained from the CD tensile test piece. The line spacing variation in this localised region was well fitted with a linear relationship, indicating a constant strain rate. The peak fitting procedure to find peak centres and the procedure of averaging 7 to 8 line spacings has significantly improved the accuracy of the obtained values compared to measuring only a single line spacing. It can be seen from Figure 4.5 that this technique is highly sensitive and the average change in line spacing between frames was 0.0052 ± 0.0003 pixels. The error was estimated from 95% confidence intervals. The strain rate was determined from the slope of the linear fit divided by the y-intercept of the fit. The measured strain rate was 0.0091% ± 0.0003% per second compared with the set strain rate of 0.0083% per second. There is thus a small difference between the experimentally measured and set strain rates. However, considering the fact that the paper is a less uniform material (i.e. local and global strain rates can differ), these results can be considered as within expectations. The most significant feature is the resolution of the technique, which is better than 0.01 pixels (0.03 μm) as can be seen from Figure 4.5.

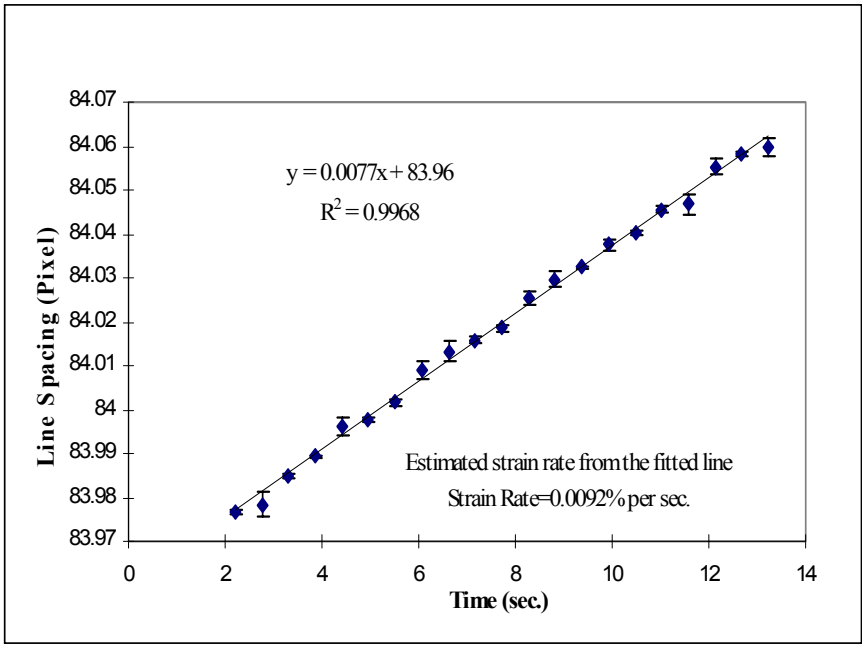

Figure 4.5 Line-spacing variation of a CD tensile test piece of copy paper with time

4.5 Plastic deformation measurements

This section presents the main measurements. First the critical load-elongation curves for the MD and CD tests are presented. These were used to determine how much to strain each sample.

4.5.1 Critical loads and displacements for DENT samples

In order to establish the load–elongation behaviour of DENT specimen under tensile load, 10 test pieces from both MD and CD direction were tested and average curves were obtained. The average load-elongation curves in CD and MD directions are showed in Figure 4.6. For the CD test, the first part of the load-elongation curve is linear (up to about 0.10 mm extension) indicating an elastic type straining. The deviation from linearity in the latter part of the curve is indicative of elastic–plastic behaviour. For the loading in the CD direction, the critical load and extension obtained just before the crack began to propagate were about 33 N and 0.5 mm respectively. For loading in the MD direction, the critical load just before crack extension was approximately 53 N and the extension was about 0.42 mm.

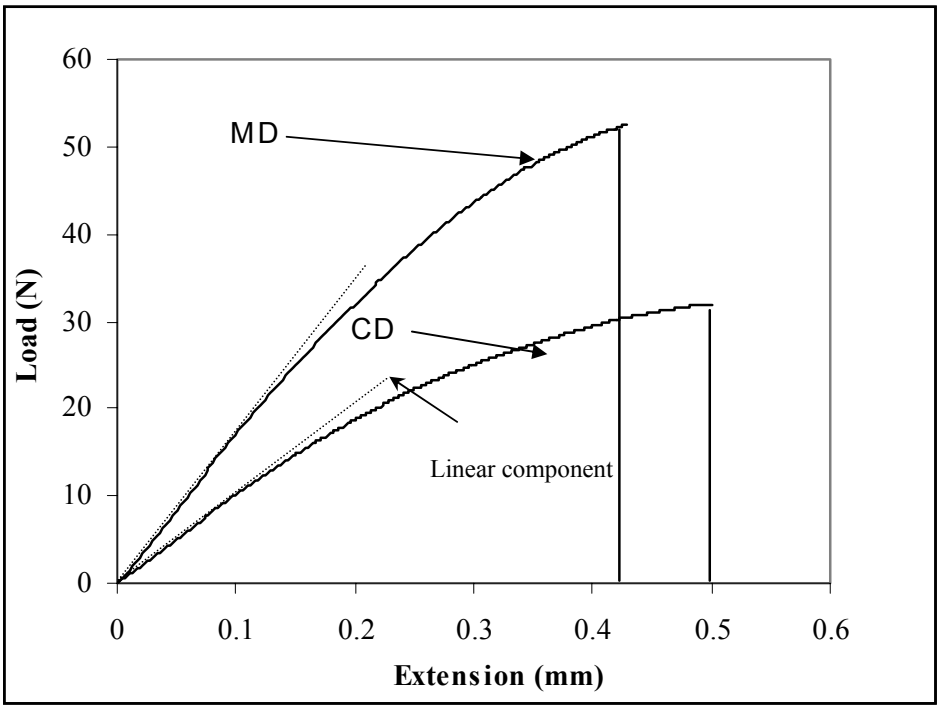

Figure 4.6. The average Load against Extension data for copy paper in the CD and MD direction for DENT test pieces. In both instances straining was stopped before crack propagation

Once the critical loads were established, the fine line printed DENT tests pieces were strained at a constant rate (2mm/min) until they reached the critical load. Real-time images of an area close to the crack-tip were captured while sample was straining (an area similar to that shown in Figure 4.2 as the ROI). The line spacing variation or strain of this region was compared with the set strain rate.

The span of the DENT test piece tested was 100 mm. A non-linear change in line spacing with time is clearly evident in the DENT test piece subjected to constant rate of elongation (see Figure 4.7). This behaviour is a result of high stress concentration at the crack-tip compared to the stress distribution in other areas of the test piece. In this case the comparison of estimated strain rate from image analysis with the set strain rate was meaningless, since the straining at the crack tip was significantly larger and also non-linear compared to the set strain rate.

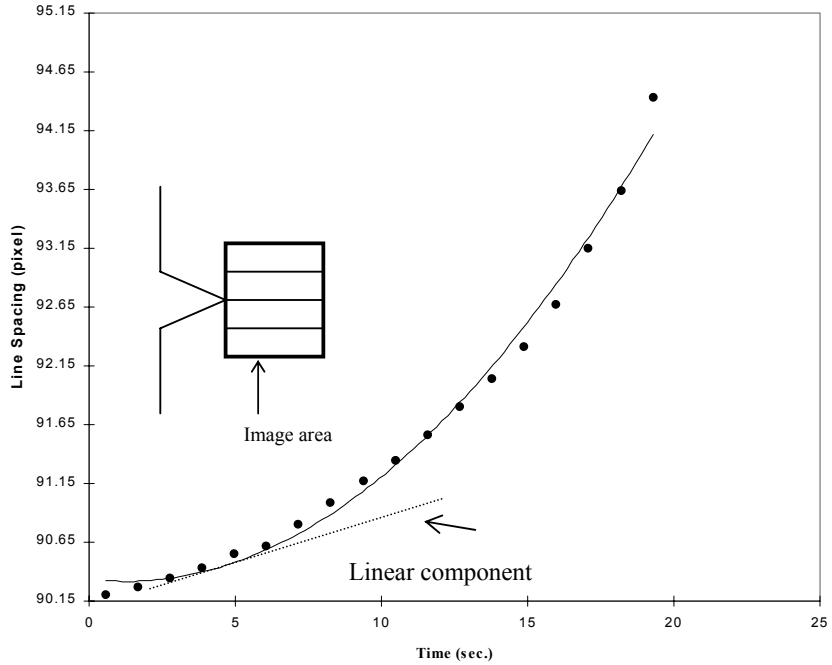

Figure 4.7. Line-spacing variation of DENT sample near the crack-tip. "Reflex" copy paper in CD direction

The next sections give the plastic deformation fields measured from the images captured from the CD and MD DENT test pieces, normal to the ligament, before and after the test pieces were strained.

4.5.2 CD DENT test piece

Figure 4.8 shows the variation in the average line spacing, in pixels, for each image captured along the first guideline in the CD direction. The x-axis gives the distance from the ligament to the centre point of the image. One data set (filled circles) shown in this figure was obtained from images captured before straining the test piece.

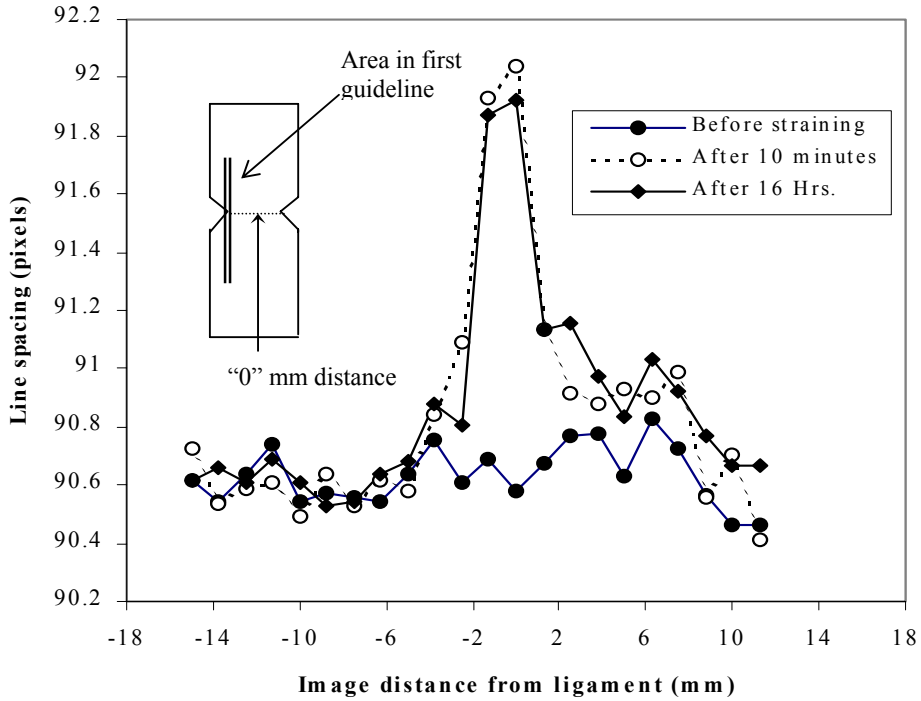

Figure 4.8. Variation of line spacing with image distance (from the ligament, along 1st guideline) for copy paper strained in the CD direction.

A second set (open circles) was obtained from images captured soon after straining. (Although image capturing was started soon after the straining, it takes about 10 to 15 minutes to complete image capture along one guideline.) A third set (filled diamonds) was obtained from the images captured after leaving the test piece at 23°C and 50% RH for nearly 16 hours after straining. This was done to examine whether there was any relaxation of the plastic strain over longer periods of time.

Although there is a reduction in the line spacing of the image located close to the middle of the ligament (0 mm distance) of the sample left for 16 hours, compared to that of sample left for 10 minutes, it is difficult to assume that this reduction was due to relaxation of the plastic strain, as this difference is most likely due to errors. This is because, while the line spacing of an individual image can be determined to better than 0.01 pixel precision, it was not possible to align the sample under the microscope to capture exactly the same area each time.

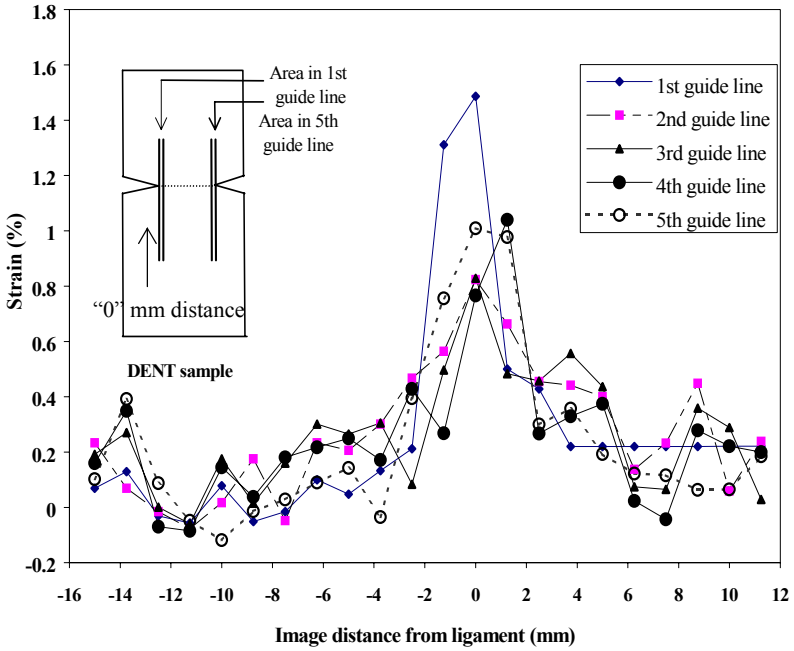

Figure 4.9. Strain (%) versus frame distance from ligament along each guideline for copy paper in CD after straining. These data were taken after 16 hours of conditioning

The maximum change in line spacing due to straining of the sample was about 1.4 pixels. This is equal to a plastic strain of 1.5 %. Figure 4.9 shows the irreversible plastic strain (%) as a function of position along the 5 guidelines normal to the ligament length. The distance from the middle of each frame to the ligament was taken as the position of the frame. The data in Figure 4.9 show that the position of maximum strain along each guideline was on the ligament (x=0) except for the data obtained along the 4^{th} guideline, where the position of maximum strain was located 1.25 mm away from the ligament position.

The strain plots in Figure 4.9 indicate that the effective deformation field estimated along guidelines 2 to 4 in the sample extended a distance of about 5mm on both sides of

the ligament. Although consistency is expected, some variation in strain is apparent in the images taken from the same distance from the ligament, along different guidelines, well away from the notch-tips. This can be seen in the way the apparent plastic strain at positions well away from the ligament varies from 0.4 % to 0.1 %. One reason for such behaviour could be due to variations in local strain fields, which can occur in a non-uniform material like paper. Another reason could be due to some variations in image location from measurement to measurement. After capture of the initial images, the test pieces were moved from the image capturing stage to the straining rig and taken back to the stage for capture of images after straining. This process introduces errors in locating the same localised position in the test piece, even though the guidelines were used. The appearance of negative strains is likely to be a consequence of such differences in the image positions when capturing images before and after straining the sample.

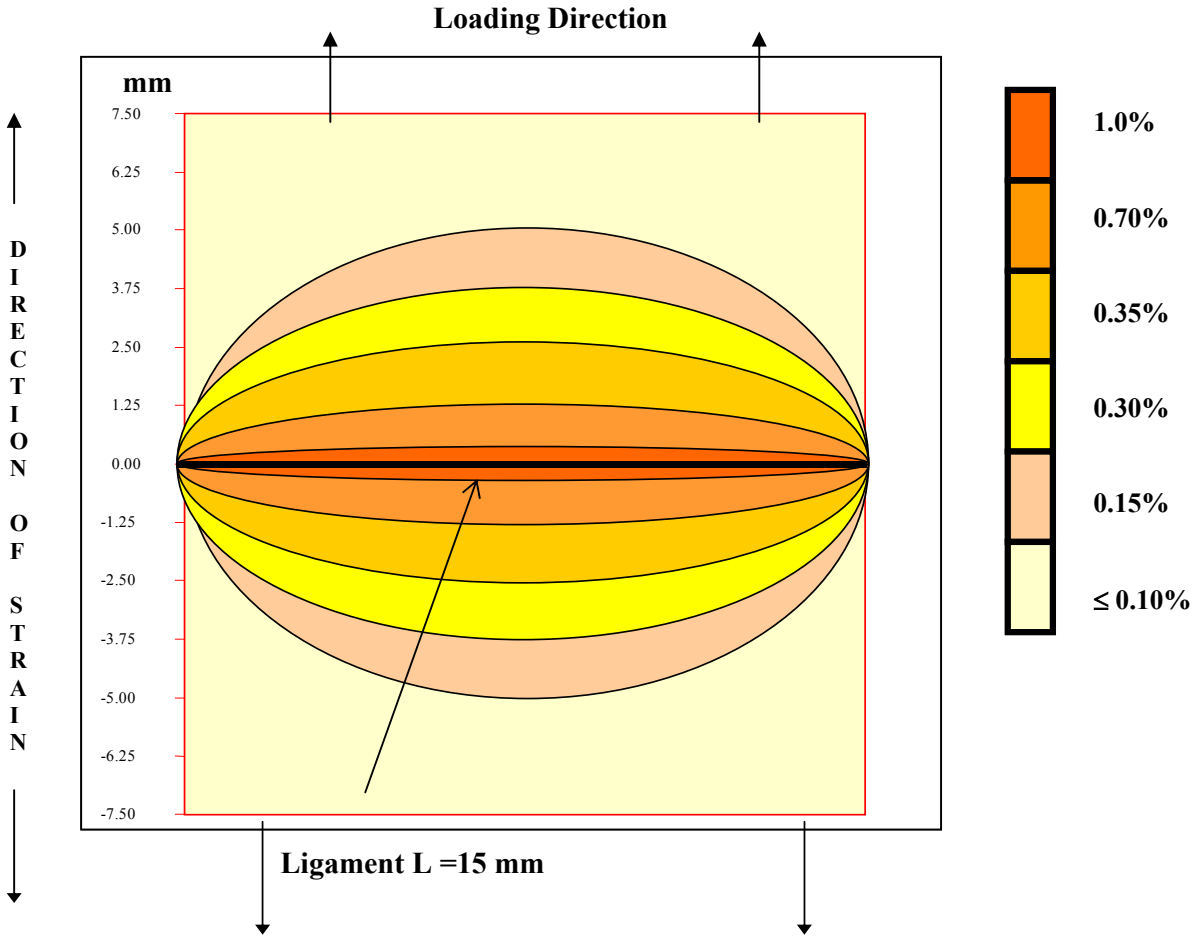

Figure 4.10. Illustration of strain profile around ligament of Reflex copy paper in CD direction

Figure 4.10 illustrates schematically the strain profile around the ligament in CD direction. This was drawn to obtain an idea about the extension of the strain field. The y-axis (in mm) is the distance from the ligament of the DENT sample to locations parallel to the ligament. Different gray scale values represent various magnitudes in strain fields. These values were obtained by averaging the strains from the same position on either side of the ligament.

Although this is not a comprehensive illustration, this strain profile provides some useful information about the spreading of the strain field and its shape. The areas with strains ≤ 0.1% are areas where no plastic strain observed. Figure 4.10 shows that the average strain (%) along the ligament (0mm distance) was 1.0%. The effective strain field has extended only a distance of 5 mm from either side of the ligament. The sharp peaks near the crack tips (as in Figure 4.9) and the 5mm extension of the effective plastic strain fields suggest that the overall strain distributions along the guidelines is more elliptical than circular. This observed strain field is not in full agreement with the assumption of the EWF technique.

4.5.3 MD DENT test piece

The line spacing in the MD test piece, showed considerable variation along the guidelines even before the sample was strained (see Figure 4.11).

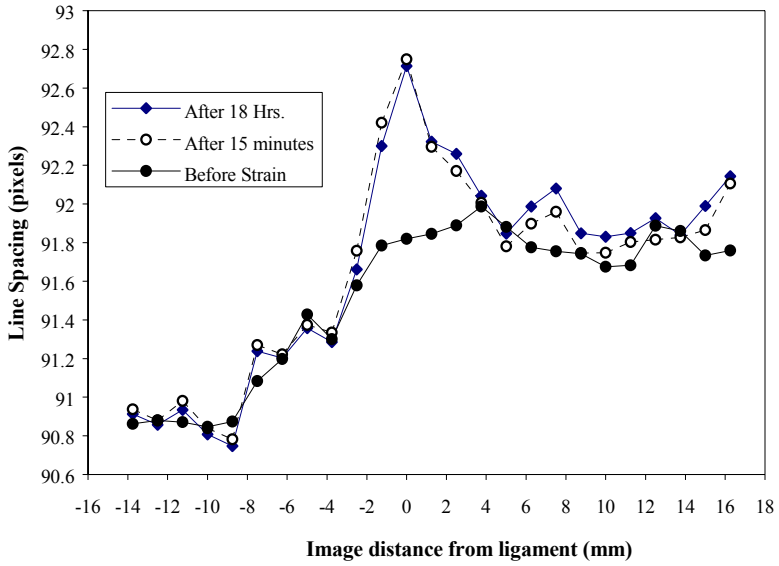

Figure 4.11. Line-spacing variation with image distance (from ligament), along 1st guideline for testing in the MD direction

This seems to be a result of the way the sample was loaded into the printer. This variation was more severe when paper was fed in the MD direction to the printer. To reduce the variation, the graphic design (fine line) generated in the computer was rotated by 90^{o}, and printed on a test piece that was fed in the CD direction to the printer. After straining, the highest magnitude of plastic strain occurs at the ligament.

The strain variation along the first three guidelines from one of the crack tips is shown in Figure 4.12. It is quite significant that no plastic strain along the second and third guidelines can be measured. This indicates that the deformation field is located only around the notches and does not extend over the whole ligament. This compares with the strain field in the CD test piece, which was approximately elliptical in shape and extended over the whole ligament length. These observations suggest that MD DENT sample with ligament L=15 mm has not fully yielded before the crack begins to propagate. This violates one of the central conditions of the EWF method.

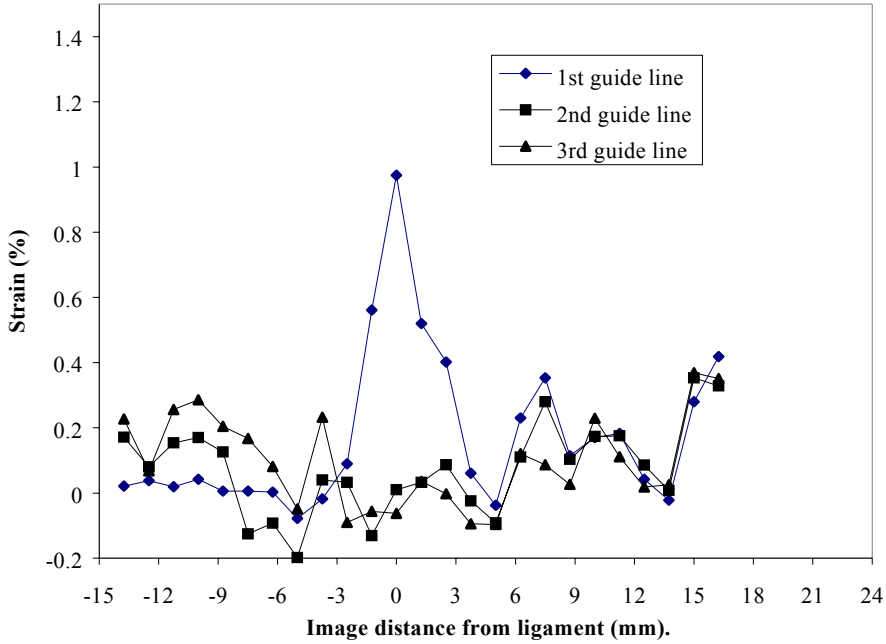

Figure 4.12. Strain (%) versus image distance (from ligament) obtained along three guidelines for copy paper in MD after straining. These data were taken after 18 hours conditioning

4.6 Estimation of plastic work in "Reflex" copy paper (CD direction)

The strain profile of the outer plastic zone obtained from the image analysis technique was used to estimate the plastic work in the outer plastic zone of the DENT sample when tested in the CD direction. The steps in the calculations were as follows:

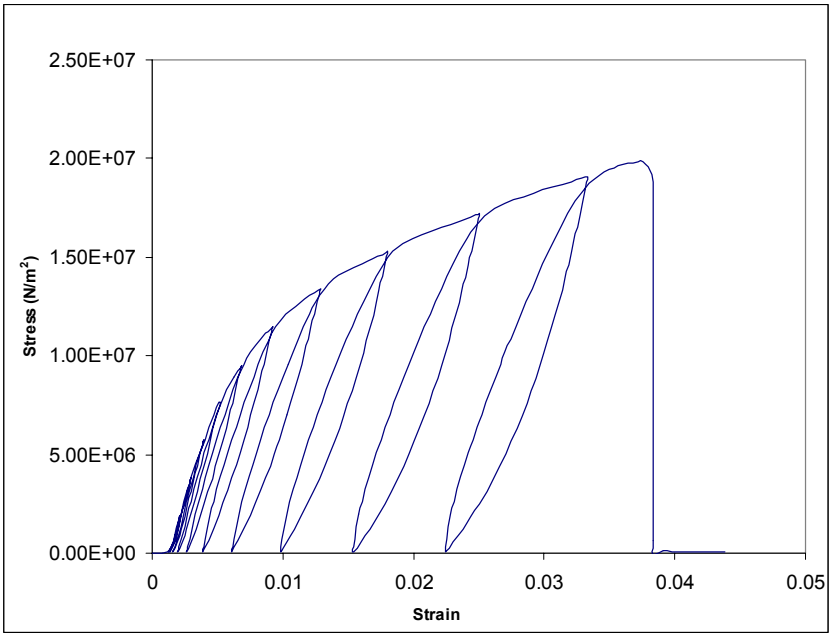

Figure 4.13. Stress versus strain of cyclically loaded tensile test piece of "Reflex" copy paper tested in the CD direction.

The first step was to estimate the work required to apply a given plastic strain to a unit area of the material. The first step in doing was to cyclically load a tensile test piece of "Reflex" copy paper in CD direction, and the maximum load in each cycle was increased from cycle to cycle in 1N increments, to obtain a load-extension curve. The strain rate was set to 2 mm /minute, which was the rate used for straining the DENT test pieces. The sample width was kept at L=15mm which was equivalent to the ligament L of the DENT sample. Also the sample length was kept similar to that of DENT sample. Figure 4.13 shows the results of this cyclic loading procedure.

The cyclically loaded stress – strain curve enables a relationship between plastic work per unit volume or "specific plastic work" and plastic strain to be constructed. There is no plastic work until the strain exceeds the elastic limit of the test piece. Thus the first data point was taken as the origin since there is no plastic work at zero plastic strain.